Available online at www.sciencedirect.com

ScienceDirect

Procedia Structural Integrity 9 (2018) 151–158

Structural Integrity Procedia

www.elsevier.com/locate/procedia

IGF Workshop "Fracture and Structural Integrity"

Evaluating the specific heat loss in severely notched stainless steel specimens for fatigue strength analyses

Daniele Rigon*, Mauro Ricotta, Giovanni Meneghetti

University of Padova, Department of Industrial Engineering, via Venezia 1 – 35131 Padova, Italy

Abstract

In the last years, a large amount of fatigue test results from plain and bluntly notched specimens made of AISI 304L stainless steel were synthetized in a single scatter band adopting the specific heat loss per cycle (Q) as a damage parameter. During a fatigue test, the Q parameter can be evaluated measuring the cooling gradient at a point of the specimens after having suddenly stopped the fatigue test. This measurement can be done by using thermocouples in the case of plain or notched material; however, due to the high stress concentration at the tip of severely notched components analysed in the present paper, an infrared camera achieving a much improved spatial resolution was adopted. A data processing technique is presented to investigate the heat energy distribution close to the notch tip of hot-rolled AISI 304L stainless steel specimens, having notch tip radii equal to 3, 1 and 0.5 mm and subjected to constant amplitude cyclic loads.

Peer-review under responsibility of the Gruppo Italiano Frattura (IGF) ExCo.

Keywords: Energy Distribution; Fatigue; Notch Effect

1. Introduction

By exploiting the surface temperature increment of the material subjected to cyclic stress, in literature some methods are reported for the rapid estimation of fatigue limit in metallic materials and components (Dengel and Harig (1980), Luong (1995), La Rosa and Risitano (2000), Curà et al. (2005)), the detection and propagation of damage in metal materials and composites in (Reifsnider and Williams (1974), Plekhov et al. (2005), Ummenhofer

* Corresponding author. Tel.: +39-049-827-6828.
E-mail address: daniele.rigon.1@phd.unipd.it

2452-3216
Peer-review under responsibility of the Gruppo Italiano Frattura (IGF) ExCo.
10.1016/j.prostr.2018.06.023

and Medgenberg (2009), Jones et al. (2010)) and the investigation of fatigue life under constant amplitude (Fargione et al. (2002), Starke et al. (2007), Jegou et al. (2013)) and block loading (Fan et al. (2012), Risitano A. and Risitano G. (2013)). The specific heat energy per cycle, Q, was assumed as a fatigue damage indicator in Meneghetti (2007), because it is expected to be a material property, similarly to the plastic strain hysteresis energy reported in Ellyin (1997).

Nomenclature

Q	specific heat loss per cycle [MJ/m^3 cycle]
c	specific heat [J/kg·K]
ρ	material density [kg/m^3]
r_n	notch tip radius [mm]
f_L	load test frequency [Hz]
f_{acq}	sampling rate [Hz]
$T(x,y)$	temperature distribution
$\overline{T}$	3-dimensional array variable of temperature images
dt	time-window variable for evaluating cooling gradient [s]
$\overline{Q}$	2-dimensional array variable of heat energy distribution
$Q(x,y)$	heat energy distribution
Q_0	specific heat loss value at the notch tip (x=0, y=0) [MJ/m^3 cycle]
$R_{Q,90\%}$	radius of biggest circular region where the energy calculated is equal or greater than 90% of Q_0 [mm]

In Meneghetti and Ricotta (2012), Meneghetti et al (2013)a, Meneghetti et al (2013)b and Meneghetti et al (2016), the Q parameter was adopted to synthesize 140 experimental results obtained from constant amplitude, push-pull, stress- or strain-controlled fatigue tests carried out on plain and notched hot rolled AISI 304L stainless steel specimens as well as from cold drawn un-notched bars of the same steel, under fully reversed axial or torsional fatigue loadings.

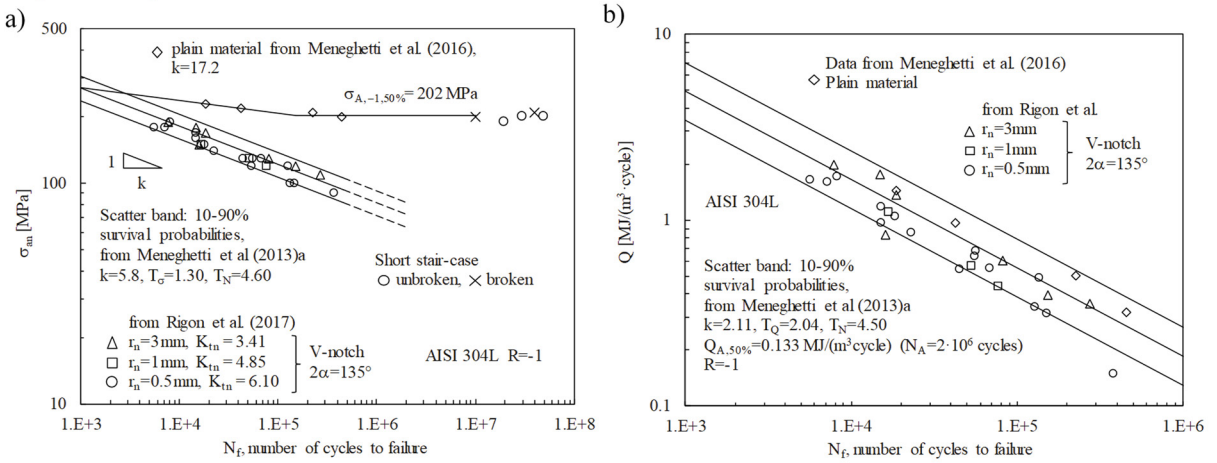

Fig. 1. Fatigue test results of plain and notched AISI 304L in term of net-section stress amplitude (a) and re-elaborated in terms of specific heat loss Q (b). Data are extrapolated from Rigon et al. (2017).

The fatigue test results synthesized in term of Q fall in a single energy-based scatter band, which was fitted only on the fatigue test results relevant to plain material, hole specimens (r_n=8 mm), U (r_n=5 mm), and bluntly V (r_n=3 mm) notched specimens (Meneghetti et al (2013)a). Depending on the severity of the stress concentration effect, the heat energy has been evaluated at a point or it has been averaged in a material volume. More precisely, in case of blunt notches, the specific heat loss has been evaluated at a point of a specimen (Q), i.e. at the notch tip; in case of

severe V-notches or cracks, the specific heat loss has been averaged in a control volume of material surrounding the tip of the stress raiser (Q*) as proposed Meneghetti and Ricotta (2016) and Meneghetti et al.(2017).

A simple experimental evaluation of the Q parameter at a point of a component's surface was proposed in Meneghetti (2007), which consists in measuring the cooling gradient at that point immediately after the fatigue test has been stopped, according to equation (1):

$$Q = \frac{\rho \cdot c \cdot \partial T / \partial t}{f_L} \tag{1}$$

where T(t) is the time-variant temperature at the point, ρ is the material density, c is the material specific heat and f_L is the load test frequency. In Meneghetti et al (2013)a, Meneghetti et al (2013)b the cooling gradients were measured by using thermocouple wires having diameter of 0.127 mm, which were attached to the notch tip by means of a 1.5-2 mm silver-loaded glue dot diameter; conversely, in Meneghetti et al (2016) and Rigon et al (2017) temperature was monitored by means of an infrared camera because of the much more localized temperature field caused by the notch tip radii lower than 3 mm, which had not been tested in Meneghetti et al (2013)a, Meneghetti et al (2013)b.

The aim of this paper is to present an automatic data processing developed in the Matlab® environment aimed to investigate the distribution of the energy dissipated around the notch tip. Such a procedure was applied to the fatigue test published in Rigon et al (2017), which are synthesised in Fig. 1. This study might be interesting for developments about energy-based approaches that needs the distribution (not only the peak) of the fatigue parameter adopted.

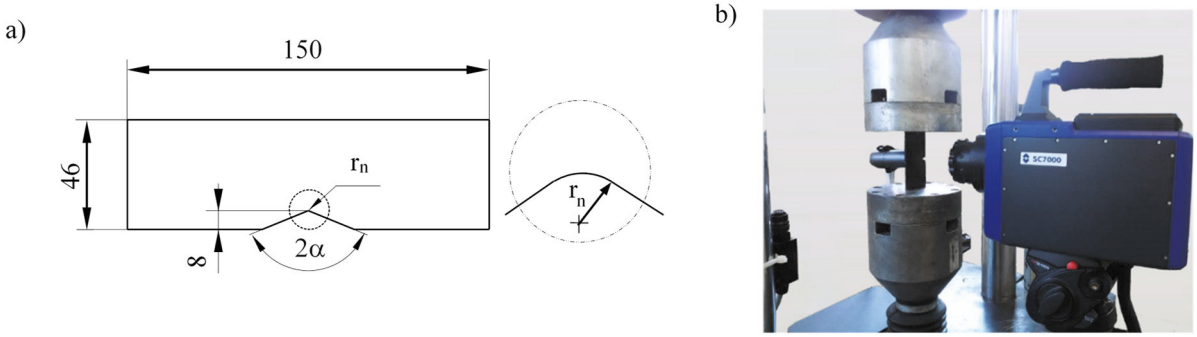

Fig. 2. Specimen's geometry (a) and experimental setup of the fatigue tests carried out in (Rigon et al. (2017)) and analyses in the present contribution (b).

2. Materials and methods

2.1. Experimental protocol

Specimens were machined from a 4-thick-mm hot rolled AISI 304L stainless steel sheet, according to the geometry shown in Fig. 2a, and considering three different notch tip radii r_n, namely equal to 3, 1 and 0.5 mm.

A FLIR SC7600 infrared camera has been adopted for recording the T(x,y) temperature maps. In order to synchronize the force and temperature signals, the infrared camera was equipped with an analog input interface. In addition, a spacer ring was used to achieve a spatial resolution around 20 μm/pixel. The frame dimension of 320x256 pixels has been set and the notch was positioned in the center of the frame to exclude the temperature error caused by vignetting. To monitor the evolution of Q during each test, 1 to 10 temperature acquisitions (before crack initiation) were performed using a 10-second-long sampling window with f_{acq}=200 Hz (2000 frames), starting from a time t_s. The time window consists of approximately 5 seconds of running test (i.e. 1000 frames between t_s and t*, Fig. 3a) followed by the machine stop at the time t*, and the remaining 5 seconds of acquisition to capture the cooling gradient (i.e. additional 1000 frames after t*). With the aim to increase the material emissivity, one

specimen's surface was black painted. On the contrary, the opposite surface was polished to detect the possible presence of a fatigue crack emanating from the notch tip, by using a AM4115ZT Dino-lite digital microscope (with a magnification ranging from 20x to 220x).

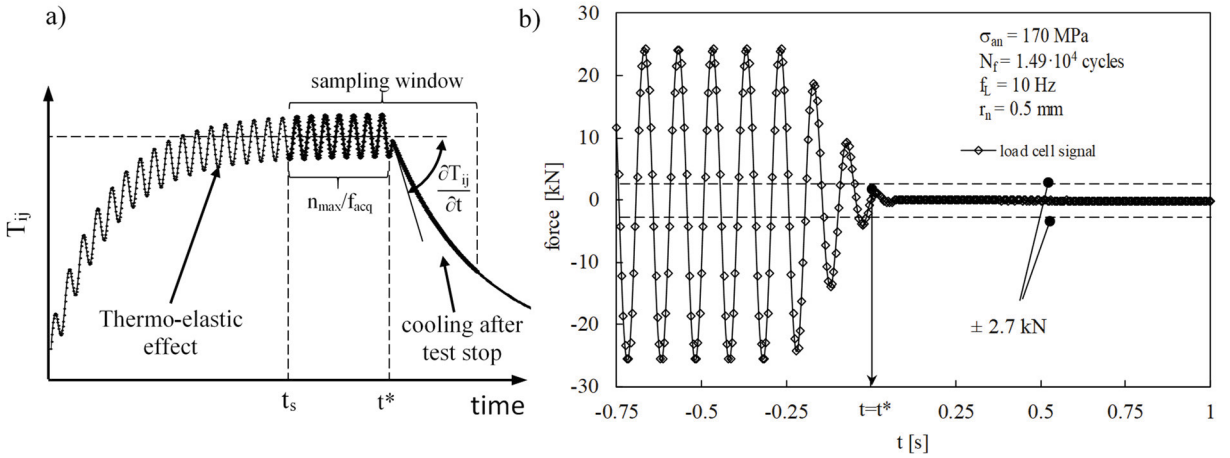

Fig. 3 .Schematic illustration of the time-variant temperature for one pixel (a) and an example of evaluation of the t* after a fatigue test stop. (b)

2.2. Data analysis

The acquired temperature maps and force signal were post-processed by means of the ALTAIR 5.90.002 commercial software and saved as Altair PTW film file (*.ptw). Since the test machine takes some tenth of a second to definitively stop, an engineering definition of t* was introduced, as follows. The time t* was defined taking advantage of the data post-processing carried out by using the ALTAIR 5.90.002 commercial software and it was defined as the time when the first peak of the tapered force amplitude signal is within the range of ±2.7 kN, i.e. below 5% of the force amplitude relevant to the fatigue test in all the acquisitions. Fig. 3b reports an example of t* evaluation.

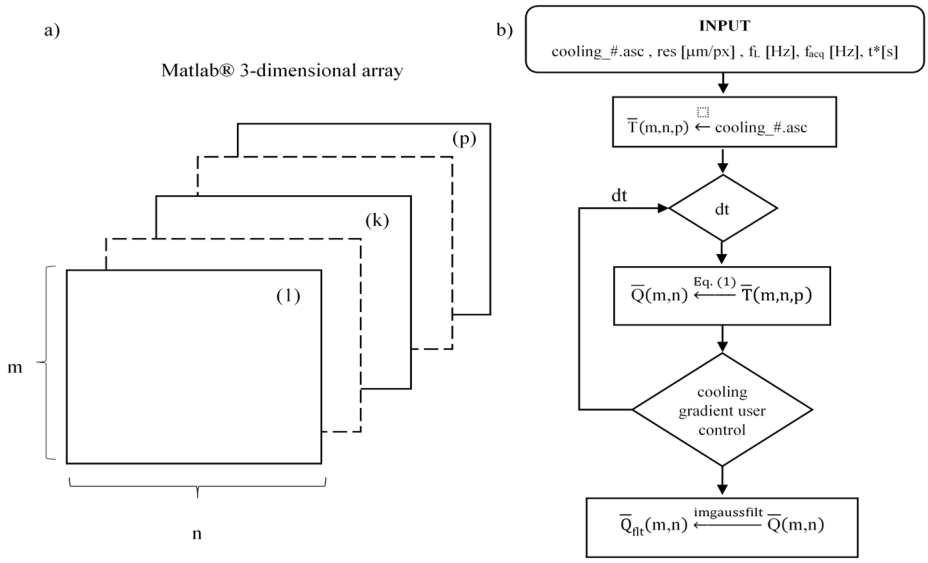

Fig. 4. Schematic representation of the 3-dimensional array $\overline{T}$ (a). Flowchart of the data analysis to obtain the energy distribution at the notch tip. (b).

In order to obtain the energy distribution at the notch tip of the considered specimens, first the Altair video recording file (*.ptw) was converted into an ASCII film file (*.asc), which is readable in Matlab. After that, the ASCII file was input to a dedicated Matlab script, that converts it into a Matlab 3-dimensional array ($\overline{T}$) having dimension m-by-b-by-p. The m, n values are the dimensions of the frame expressed in terms of pixels, reduced to avoid vignetting (m=136 px, n=167 px), and p is the number of frames acquired by the infrared camera (i.e p is equal to 2000). A schematic illustration of $\overline{T}$ script is shown in Fig. 4a. Let i, j and k be the indexes of $\overline{T}$. An element of this 3D array corresponds to a temperature value of the n-th pixel having coordinate i and j for the k-th frame. In this way, fixing i and j and plotting T_{ij} against the time (obtained from the division of the k index value by f_{acq}), the time variant temperature graph, commonly used for evaluated the Q parameter, is obtained for the n-th pixel.

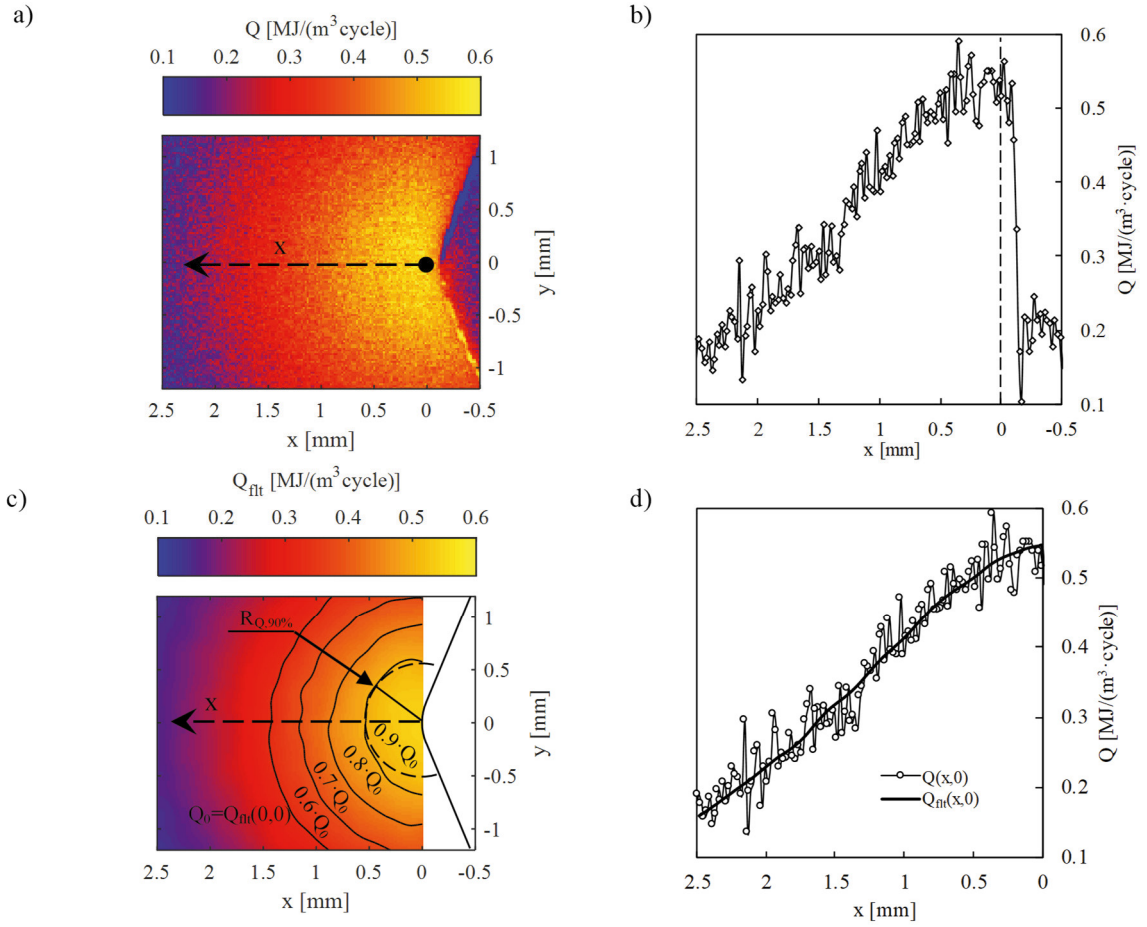

Fig. 5. Example of raw data of the energy distribution Q(x,y) (a) and along the coordinate y=0 (along the notch bisector (b). The filtered energy distribution $Q_{flt}(x,y)$ (c) and the relevant distribution along the notch bisector (y=0) (d). (a-d) data are referred to the acquisition obtained at N = $8.12 \cdot 10^3$ cycles of the specimen characterised by r_n=0.5 mm, σ_{an}=130 MPa, and $N_f = 6.76 \cdot 10^4$.

A time window equal to 0.1s was tentatively assigned to a numerical variable, named “dt”, for evaluating the cooling gradient of the n-th pixel and it was kept constant for all pixels (see Fig. 4b). In practice, the numerical evaluation of the cooling gradient was performed by the *polyfit* matlab function, which returns the value of the slope of the linear fitting of the data within the value of dt, then Q_{ij} is evaluated applying Eq. (1). This operation was routinely performed for all pixels by a *for loop*, resulting in a m-by-n matrix composed by Q_{ij} values, called $\overline{Q}$. Having the same dt value fixed for all the pixels and a certain level of noise in the measurements, the cooling gradient might result meaningless for some pixels. Therefore, after plotting the $\overline{Q}$ matrix, a check was performed to single-out unrealistic spike-like values. Then, the dt value was iteratively modified in the range from 0.05 s to 0.15 s

in order to eliminate the aforementioned spike-like Q_{ij} values. Once passed this control, the last step consisted in filtering the 2-D matrix $\overline{Q}$ adopting a matlab function called *imgaussfilt*, which uses a Gaussian smoothing kernel with specified standard deviation. For this application, a standard deviation ranging from 4 to 6 was adopted.

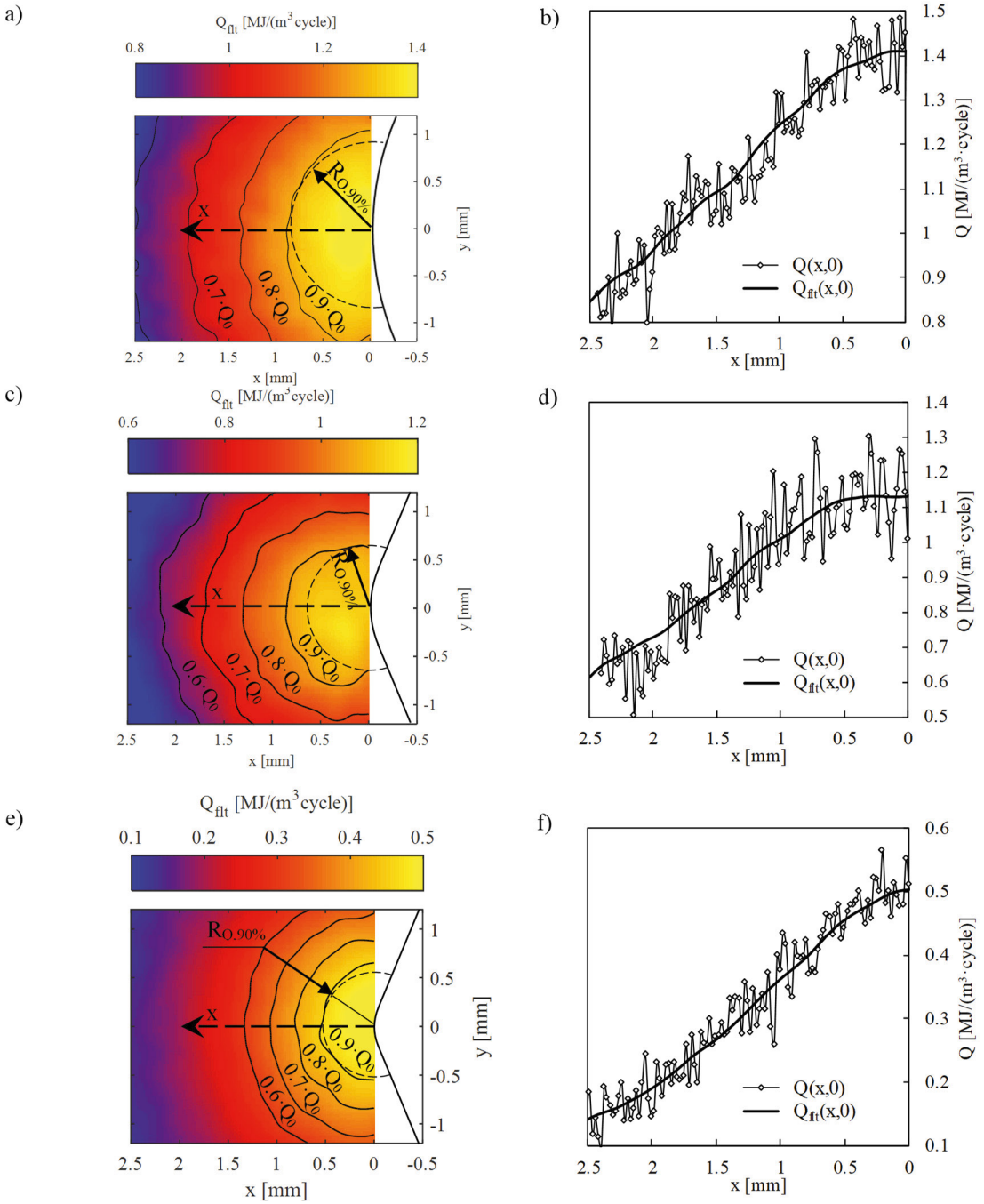

Fig. 6. Heat energy distributions at the notch tip: (a,b,) rn=3 mm, σan=170 MPa, Nf=1.85·104 cycles; (c,d) rn=1 mm, σan=150 MPa, Nf=1.67·104 cycles; (e,f) rn=0.5 mm, σan=100 MPa, Nf=1.35·105 cycles

The matrix variable obtained is called $\overline{Q}_{flt}$. Due to the well-known difficulty of detecting the edges in thermography, a scratch was made on the painted surface of the specimens. The distance of this scratch from the

notch tip was measured by the digital microscope before each fatigue test, in order to find the position of the notch tip (x=0 and y =0) in the thermal image and also to define the actual resolution (μm/pixels) of each experimental test and it was stored in a variable called "res" (see Fig.4b). Having the resolution, a grid of metric coordinates was created by the matlab function called *meshgrid*, allowing to plot the energy distribution with a metric coordinate system centered at the notch tip. Furthermore, the negative portion of images was removed ($x < 0$) to exclude the edges of the notch form the final results. In summary, the computational phases of the heat energy distribution analysis are synthesised as flowchart in Fig. 4b.

3. Results: Q fields at the notch tip

Fig. 5a shows an example of the Q(x,y) raw data measured at $N = 8.12 \cdot 10^3$ for a specimen with $r_n = 0.5$ mm subjected to σ_{an}=130 MPa ($N_f = 6.76 \cdot 10^4$ cycles), whereas the distribution Q(x,0) along the notch bisector is reported in Fig. 5b. As it was mentioned in the previous section, the results are affected by a certain level of noise because the dt variable was maintained constant for all the pixels of the thermal images.

Fig. 5c shows the filtered results ($Q_{flt}(x,y)$) for the same example, and in Fig. 5d, the comparison between Q(x,0) and $Q_{flt}(x,0)$ along the notch bisector is reported.

In addition, constant energy contours normalized with respect to Q_0, which is define as the energy dissipated at the notch tip (i.e $Q_{flt}(0,0)$), are reported in Fig. 5c. It is worth noting that in Fig. 5c the iso-energy contours seem to be circular and centered at the not tip. In particular, a circular contour with radius $R_{Q,90\%}$ has been plotted in order to identify the biggest region where the energy calculated is equal or greater than 90% of Q_0. For the example reported in Fig. 5c $R_{Q,90\%}$ is equal to 0.54 mm.

Fig. 6 shows more examples of energy distribution Q(x,y) and the relevant distribution along the notch bisector Q(x,0), for different notch tip radii and applied stress amplitudes.

The evaluation of the $R_{Q,90\%}$ has been carried out on selected specimens and the results are summarized in Table 1. Although the estimates of $R_{Q,90\%}$ ranges from 0.53 to 0.87 mm, there may be a link between $R_{Q,90\%}$ and the structural volume size for fatigue strength assessment evaluated in a recent work (Meneghetti et al (2017), Meneghetti and Ricotta (2018)) for the same material and testing condition, but more investigation should be carried out.

Table 1. Value of radius RQ,90% measured during the fatigue test.

r_n [mm]	σ_{an} [MPa]	f_L [Hz]	N_f	N^*/N_f	Q_0 [MJ/(m^{3}cycle)]	$R_{Q,90\%}$ [mm]	N/Nf
3	190	10	$7.82 \cdot 10^3$	0.41	1.98	0.85	0.24
3	170	10	$1.85 \cdot 10^4$	0.61	1.45	0.87	0.42
3	110	25	$2.71 \cdot 10^5$	0.67	0.38	0.55	0.17
1	150	10	$1.67 \cdot 10^4$	0.33	1.17	0.64	0.28
1	120	15	$7.68 \cdot 10^4$	0.40	0.42	0.55	0.13
0.5	190	5	$8.17 \cdot 10^3$	0.40	1.77	0.83	0.21
0.5	100	35	$1.35 \cdot 10^5$	0.13	0.51	0.53	0.08
0.5	130	25	$6.76 \cdot 10^4$	0.22	0.55	0.54	0.12

4. Conclusions

In the present contribution, an automated procedure is proposed to evaluate the specific heat loss (Q parameter) distribution around sharp V-notches, starting from the temperature maps captured around the tip of V notches, by using an infrared camera having a geometric resolution equal to 20 μm/pixel. Fully reversed, constant amplitude fatigue tests were carried out on 4-mm-thick AISI 304L stainless steel specimens having a lateral V-notch, with notch tip radii equal to 3, 1 and 0.5 mm and opening angle of 135°.

The automated procedure was developed in Matlab® code taking the video recording file acquired by ALTAIR 5.90.002 commercial software as input file and computing Eq (1) pixel-by-pixel. Then Q distributions (Q(x,y)) were

analysed for a subset of specimens providing the circular region where the energy dissipated is equal or greater of 90% of the Q value measured at the notch tip. By considering the material and the test conditions analysed in the present paper, it can be concluded that Q can be considered practically constant at least from an engineering point of view in within a circular region centered at the notch tip and having a radius ranging from 0.53 to 0.83 mm.

Acknowledgements

This work was carried out as a part of the project CODE CPDA145872 of the University of Padova. The Authors would like to express their gratitude for financial support.

References

Curà, F., Curti, G., Sesana, R., 2005. A new iteration method for the thermographic determination of fatigue limit in steels, International Journal of Fatigue 27, 453–459.

Dengel, D., Harig, H., 1980. Estimation of the fatigue limit by progressively-increasing load tests, Fatigue & Fracture of Engineering Materials & Structures 3, 113–128.

Ellyin, F., 1997. Fatigue damage, crack growth, and life prediction, Chapman & Hall.

Fan, J., Guo, X., Wu, C., 2012. A new application of the infrared thermography for fatigue evaluation and damage assessment, International Journal of Fatigue 44, 1–7.

Fargione, G., Geraci, A., La Rosa, G., Risitano, A., 2002. Rapid determination of the fatigue curve by the thermographic method, International Journal of Fatigue 24, 11–19.

Jegou, L., Marco, Y., Le Saux, V., Calloch, S., 2013. Fast prediction of the Wöhler curve from heat build-up measurements on Short Fiber Reinforced Plastic, International Journal of Fatigue 47, 259–267.

Jones, R., Krishnapillai, M., Cairns, K., Matthews, N., 2010. Application of infrared thermography to study crack growth and fatigue life extension procedures, Fatigue & Fracture of Engineering Materials & Structures 33, 871–884.

La Rosa, G., Risitano, A., 2000. Thermographic methodology for rapid determination of the fatigue limit of materials and mechanical components, International Journal of Fatigue 22, 65–73.

Luong, M.P., 1995. Infrared thermographic scanning of fatigue in metals, Nuclear Engineering and Design 158, 363–376.

Meneghetti, G., 2007. Analysis of the fatigue strength of a stainless steel based on the energy dissipation, International Journal of Fatigue 29, 81–94.

Meneghetti, G., Ricotta, M., 2012. The use of the specific heat loss to analyse the low- and high-cycle fatigue behaviour of plain and notched specimens made of a stainless steel, Engineering Fracture Mechanics 81, 2–16.

Meneghetti, G., Ricotta, M., 2016 Evaluating the heat energy dissipated in a small volume surrounding the tip of a fatigue crack, International Journal of Fatigue 92, 605–615.

Meneghetti, G., Ricotta, M., 2018 The heat energy dissipated in the material structural volume to correlate the fatigue crack growth rate in stainless steel specimens, International Journal of Fatigue, under review.

Meneghetti, G., Ricotta, M., Atzori, B., 2013. A synthesis of the push-pull fatigue behaviour of plain and notched stainless steel specimens by using the specific heat loss, Fatigue & Fracture of Engineering Materials & Structures 36, 1306–1322.

Meneghetti, G., Ricotta, M., Atzori, B., 2016. The heat energy dissipated in a control volume to correlate the fatigue strength of bluntly and severely notched stainless steel specimens, Proceedings of the 21st European Conference on Fracture, ECF21, Catania, Italy, Procedia Structural Integrity 2, 2076–2083.

Meneghetti, G., Ricotta, M., Rigon, D., 2017. The heat energy dissipated in a control volume to correlate the fatigue strength of severely notched and cracked stainless steel specimens, Proceedings of International Fatigue Conference, Cambridge, UK.

Meneghetti, G., Ricotta, Negrisolo, L., Atzori, B., 2013. A synthesis of the fatigue behavior of stainless steel bars under fully reversed axial or torsion loading by using the specific heat loss, Key Engineering Materials 577–578, 453–456.

Plekhov, O., Palin-Luc, T., Saintier, N., Uvarov, S., Naimark, O., 2005. Fatigue crack initiation and growth in a 35CrMo4 steel investigated by infrared thermography, Fatigue & Fracture of Engineering Materials & Structures 28, 169–178.

Reifsnider, K.L., Williams, R.S., 1974. Determination of fatigue-related heat emission in composite materials, Experimental Mechanics 14, 479–485.

Rigon, D., Ricotta, M., Meneghetti, G., 2017. An analysis of the specific heat loss at the tip of severely notched stainless steel specimens to correlate the fatigue strength, Theor. Appl. Fract. Mech. 92, 240–251

Risitano, A., Risitano, G., 2013. Cumulative damage evaluation in multiple cycle fatigue tests taking into account energy parameters, International Journal of Fatigue 48, 214–222.

Starke, P., Walther, F., Eifler, D., 2007. Fatigue assessment and fatigue life calculation of quenched and tempered SAE 4140 steel based on stress–strain hysteresis, temperature and electrical resistance measurements, Fatigue & Fracture of Engineering Materials & Structures 30, 1044–1051.

Ummenhofer, T., Medgenberg, J., 2009. On the use of infrared thermography for the analysis of fatigue damage processes in welded joints, International Journal of Fatigue 31, 130–137.